

1. Introductory review and technical approaches

MARTIN M. ROTH

1.1 Preface

The topic of the XVII IAC Winter School is ‘3D Spectroscopy’: a powerful astronomical observing technique, which has been in use since the early stages of the first prototype instruments about a quarter of a century ago. However, this technique is still not considered a standard common user tool among most present-day astronomers.

3D Spectroscopy (hereafter ‘3D’) is also called ‘integral field spectroscopy’ (IFS), sometimes ‘two-dimensional’ or even ‘area’ spectroscopy, and commonly also ‘three-dimensional’ spectroscopy; in other areas outside astronomy it is called ‘hyperspectral imaging’, and so forth. It is already this diversity in the nomenclature that perhaps reflects the level of confusion. For practical reasons, the organizers of this Winter School and the Euro3D network (which will be introduced below) have adopted the terminology ‘3D’, which is intuitively descriptive, but, as a caveat early on, is conceptually misleading if we restrict our imagination to the popular picture of the ‘datacube’ (Figure 1.1). Although this term will commonly be used throughout this book, we need to point out for the reasons given later in the first chapter that the idealized picture of an orthogonal cube with two spatial, and one wavelength, coordinate(s) is inappropriate in the most general case.

Whatever the terminology, it is the aim of this Winter School to help alleviate the apparent lack of insight into 3D instrumentation, its use for astronomical observations, the complex problems of data reduction and analysis, and to spread knowledge among a significant number of international young researchers at the beginning of their career. The training of early stage researchers has always been the rationale in the tradition of the well-established series of Instituto de Astrofísica de Canarias (IAC) Winter Schools, but this is the first time in which a consortium of 11 leading European research institutes appears as co-organizer, represented by the ‘Euro3D’ Research Training Network (RTN) – which may well be recognized as the significant impact expected from this school. Euro3D was funded by the European Commission (EC) from July 2002 to December 2005 under Framework Programme 5 (Walsh and Roth, 2002). The RTN participants are as follows:

- Astrophysikalisches Institut Potsdam (Germany, coordinator)
- IoA University of Cambridge (UK)
- Durham University (UK)
- MPE Garching (Germany)
- European Southern Observatory (International Organization)
- Sterrewacht Leiden (The Netherlands)
- Observatoire de Lyon (France)
- CNRS Marseille (France)
- IFCTR Milano (Italy)
- Observatoire de Paris, Meudon (France)
- IAC Tenerife (Spain).

At the time of planning the RTN in 2001, these groups represented practically the entire expertise in 3D instrumentation in Europe. As can be seen from a compilation of existing instruments and those under development at the time (Table 1.1), significant capital

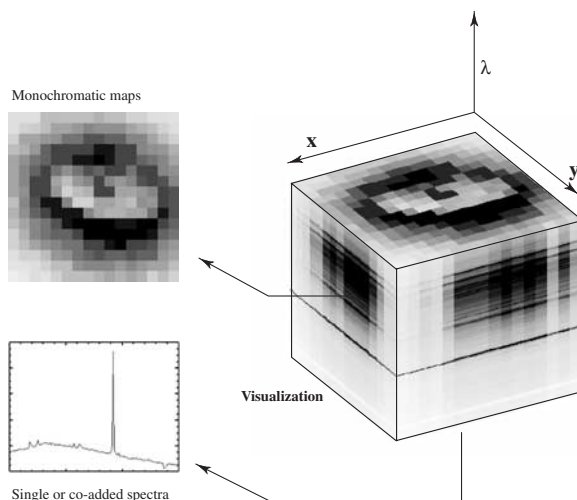


FIGURE 1.1. Schematic representation of a datacube, produced as the result of 3D observations. It can be interpreted as a stack of quasi-monochromatic images or, alternatively, as an assembly of $n \times m$ spectra.



FIGURE 1.2. Participants of the Euro3D Kickoff Meeting, held at IAC, Tenerife, 2–4 July 2002.

investments have been realized at almost all major observatories, with a clear technological lead in Europe. Disappointingly, however, the expertise within the user community for the reception of the data from such instruments was found to be very limited. It was confined almost entirely to members of the groups that have built the 3D instruments.

Therefore, and in response to the EC requirement to demonstrate ‘the scientific, technological, or socio-economic reasons for carrying out research in the field covered by the network’, the project objectives of the Euro3D consortium were identified as follows:

- to promote 3D technique with selected science projects
- to develop new observing and data reduction techniques
- to provide training and education of students and young researchers
- to popularize 3D technique in various research fields
- to provide user support and general information

TABLE 1.1. Compilation of 3D instrumentation on some major telescopes (as of 2001). Notes: Bold face: 3D instruments built by RTN members. (●): facilities accessible through Euro3D. ¹⁾: mobile instrument.

Telescope	Diameter (m)	Access Euro3D	3D Instrument	$\Delta\lambda$ (μm)	Maximum FoV arcsec ²	Maximum resolution $\lambda/\Delta\lambda$	Status
NGST	8.0	●	IFMOS				proposed
HST	2.4	●	–				
Keck	2 × 10		OSIRIS	0.9–2.5	3 × 6	4000	planned
GTC	10	●	ATLANTIS	1–2.4	8 × 8	5000	planned
HET	10		–				
LBT	2 × 8.4	●	PMAS ¹⁾	0.35–1.0	16 × 16	2200	private
SUBARU	8.3		Kyoto-3D				
GEMINI	2 × 8.1	●	GMOS	0.4–1.0	50 × 450	10000	common user
		●	GNIRS	1–5	20 × 20	5000	common user
		●	CIRPASS	0.9–1.8	35 arcsec ²	3000	common user
		●	NIFS	1–2.5	3 × 3	5300	planned
VLT	4 × 8.1	●	VIMOS	0.37–1	54 × 54	2000	common user
		●	NIRMOS	1–1.8	28 × 28	2500	common user
		●	SINFONI	1–2.5	8 × 8	4500	common user
		●	FLAMES	0.37–0.9	11.5 × 7.3	25000	common user
Magellan	2 × 6.5	●	IMACS	0.4–0.9	50 × 50	5000	common user
Selentchuk	6.0	●	MPFS	0.39–0.9	16 × 16	3000	common user
Hale	5.0		PIFS	1–5	5.4 × 9.6	3000	experimental
WHT	4.2	●	INTEGRAL	0.39–1.0		1800	common user
		●	SAURON	0.47–0.54	39.5 × 32.9	2300	private
		●	TEIFU	0.47–0.54	4.1 × 5.9		private
CTIO	4.0		–				
KPNO	4.0		–				
AAT	3.9	●	SPIRAL	0.48–1.0	22 × 11	11000	'expert' user
CFHT	3.6	●	TIGER	0.4–1.0	12 × 9	2000	decommissioned
		●	OASIS	0.4–1.0	15 × 12	3000	common user
ESO 3.6 m	3.6	●	–				
WYIN	3.5		DENSEPAK	0.38–1.0	90 fibers	22000	common user
Calar Alto	3.5	●	PMAS ¹⁾	0.35–1.0	16 × 16	2200	private
NTT	3.5	●	–				
TNG	3.5	●	GOHSS	0.8–1.8		3000	planned
		●	MPE-3D ¹⁾	1.5–2.2	6.4 × 6.4	2100	private



FIGURE 1.3. The conceptually problematic picture of a ‘datacube’

- to provide feedback from observers to technology
- to identify technology transfer opportunities.

Organizing the XVII IAC Winter School is an important contribution to its major goals and appropriately concludes the activities at the end of the lifetime of the RTN. It is hoped that the participants of the Winter School will benefit from the collective expertise presented in the lectures for the rest of their future scientific careers; furthermore that 3D Spectroscopy shall experience more widespread use in the community to further exploit and advance its unique potential for astronomy.

1.2 Introductory review

1.2.1 *Conceptual outline*

Principle of operation and terminology

We define integral field (3D) spectroscopy (IFS) as an astronomical observing method that creates in a single exposure spectra of (typically many) spatial elements (‘spaxels’) simultaneously over a two-dimensional field-of-view (FoV) on the sky. Owing to this sampling method, each spaxel can be associated with its individual spectrum. Once all of the spectra have been extracted from the detector frame in the process of data reduction, it is possible to reconstruct maps at arbitrary wavelengths. For instruments with an orthonormal spatial sampling geometry, the spectra can be arranged on the computer to form a three-dimensional array, which is most commonly called a ‘datacube’. Datacubes are also well known as the natural data product in radio astronomy. Note, however, that there are many integral field spectrographs which do not sample the sky in an orthonormal system. In this case the term datacube is misleading. We shall see further below that atmospheric effects in the optical also make the term inappropriate in the most general case.

Historically, various designations have been invoked to describe integral field spectroscopy (area/imaging/2D/3D/three-dimensional spectroscopy, etc.). As spectroscopy involves one dimension per se (the wavelength scale), two-dimensional spectroscopy would arguably also describe the situation correctly. However, the datacube picture and the perhaps more explicit label ‘3D’ have conventionally led to the now accepted terminology of three-dimensional spectroscopy, which is adopted throughout this book.

Instruments that create three-dimensional datasets in the sense described above, however not simultaneously but rather in some process of sequential data acquisition (scanning), e.g. tuneable filter (Fabry–Perot) instruments, scanning long slits, etc., are not strictly 3D spectrographs according to our definition. Because of similarities in the

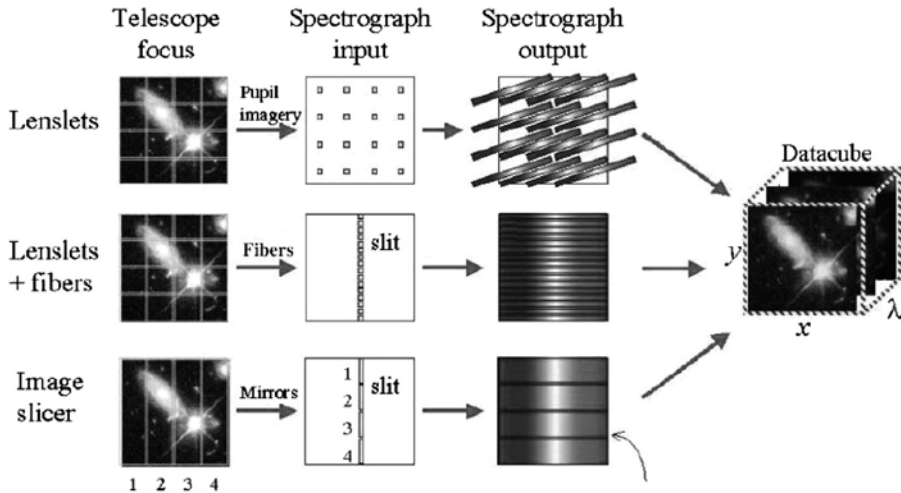


FIGURE 1.4. The three major principles of operation of present-day IFUs (Source: J. Allington-Smith).

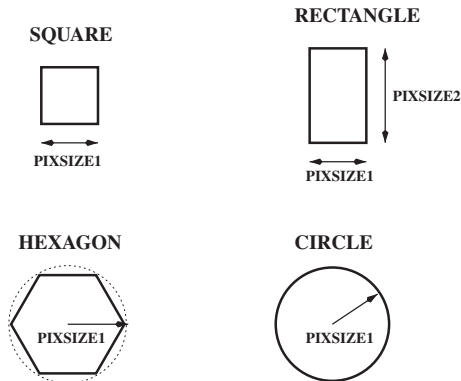


FIGURE 1.5. Different types of spaxel geometries: square, rectangular, hexagonal, bare fiber (circular).

analysis and interpretation of their data, however, such instruments will also be mentioned briefly below.

Methods of image dissection: spatial sampling

Integral field spectrographs have been built based on different methods of dissecting the FoV into spaxels, e.g. optical fiber bundles, lens arrays, optical fibers coupled to lens arrays, or slicers (Figure 1.4). We will discuss these methods further below.

The term ‘spaxel’ was introduced by the Euro3D consortium in order to distinguish spatial elements in the image plane of the telescope from pixels, which are the spatial elements in the image plane of the detector (Kissler-Patig *et al.*, 2004). The optical elements that accomplish the sampling of the sky are often called ‘integral field units’ (IFUs), and thus IFS is also sometimes called ‘IFU spectroscopy’. Spaxels can have different shapes and sizes, depending on instrumental details and the type of IFU (Figure 1.5).

It is necessary to point out that, contrary to the persuasive implication of the datacube picture, IFUs do not necessarily sample the sky on a regular grid, e.g. fiber bundles, where

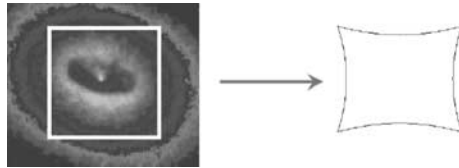


FIGURE 1.6. Field distortion in the fore-optics of an IFU affects the spatial sampling.

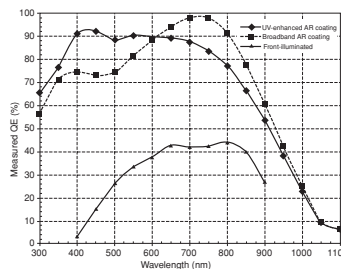


FIGURE 1.7. Fairchild CCD 4K × 4K, 15 μm pixels (left). The QE of modern CCDs can be made quite high, very nearly approaching 100% (right).

due to the manufacturing process individual fibers cannot be arranged to arbitrary precision (for a real fiber bundle IFU, see Figure 1.23). This is another reason why the popular description of IFS as ‘like a CCD [charge coupled device] with a spectrum in each pixel’ is misleading. Even if the manufacture of an IFU allows a perfectly regular sampling pattern to be created, e.g. in the case of a hexagonal lens array, the sampling is not necessarily orthonormal. Moreover, real optical systems create aberrations and, sometimes, non-negligible field distortions (Figure 1.6), which also means that the set of spectra extracted from the detector does not sample an orthogonal FoV on the sky. Furthermore, the sampling method may be contiguous (e.g. lens array) with a fill factor very close to unity, or non-contiguous (e.g. fiber bundle) with a fill factor of significantly less than 100%. In all of these cases, it is possible to reconstruct maps at a given wavelength through a process of interpolation and, repeating this procedure over all wavelengths, to convert the result into a datacube. Note, however, that interpolation often produces artifacts and generally involves loss of information.

Detectors and spectrographs

In order to better understand the potential and natural constraints of 3D instrumentation, it is useful to briefly review detectors, since they ultimately limit the total number of spatial and spectral resolution elements, hence FoV and wavelength coverage. Depending on the type of application, one would normally try to maximize the number of detector pixels in order to maximize one or both of these parameters. A selection of modern large area detectors is illustrated below. For visual wavelengths in the interval 0.35–1.0 μm, CCDs are nowadays the most common detectors, featuring high quantum efficiency (QE) and low read-out noise. Single chips with pixel resolutions of 4096 × 4096 (Figure 1.7) presently represent the state-of-the-art, although much larger CCDs are under development. In order to obtain even larger pixel numbers, butttable CCDs can be arranged to form mosaic configurations similar to modern wide-field imaging cameras (MegaCAM, OmegaCam, etc.), e.g. the detector for the IMACS IFU (Inamori Magellan Cassegrain Spectrograph – Integral Field Unit), which is built as a mosaic of 2 × 3 2K × 4K CCD chips. Image-intensified photon counting detectors that were still common in the 1980s

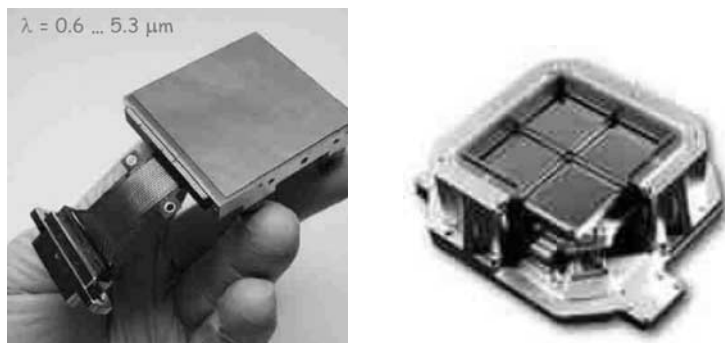


FIGURE 1.8. Rockwell 2K × 2K Infrared Array (left), 4K × 4K mosaic (right).

are no longer popular, except for read-noise limited applications with very low photon count rates. An interesting new development is the photon-counting LLCCD, which uses an on-chip avalanche gain technology for low noise at high frame rates (Jerram *et al.*, 2001).

In the near infrared (NIR) wavelength regime there has been enormous progress in detector technologies, providing large area infrared (IR) arrays with pixel resolutions of up to 2K × 2K and excellent electro-optical performance, and even larger arrays being under development. A mosaic of 2 × 2 such butttable arrays is shown in Figure 1.8. While a strong driver for this evolution has come from the development of the next generation space telescope – the James Web Space Telescope (JWST) – it is also the demand for detectors from NIR instrumentation for ground-based astronomy that has made NIR astronomy a rapidly growing field.

The number of spectra delivered by present-day 3D spectrographs is typically in the range of several hundreds up to a few thousand: Visible Imaging Multi-Object Spectrograph (VIMOS) IFU: 6400 (Le Fevre *et al.*, 2003). The corresponding number of spaxels is disappointingly small if one compares with direct imaging detectors: even the simple first generation commercial CCD imagers were offering, for example, $384 \times 576 \approx 221$ Kpixels: a factor of 34 larger than the number of spaxels of the largest IFU to date. So what is it that limits the size of an integral field spectrograph in terms of number of spatial and spectral elements?

First of all, IFS is obviously more complex than direct imaging: for any spatial element, a full spectrum must be accommodated. If n , m , k are the number of spatial resolution elements in x and y , and of the spectral resolution elements, respectively, then the total number N of required detector pixels is $N = n \times m \times k$. In comparison with direct imaging where $k = 1$, IFS requires at least a factor of k more detector pixels. Clearly, instrumentation for IFS is expensive in terms of detector space.

Another important factor is the spectrograph optical system. The input focal ratio as determined by the telescope and any fore-optics, the magnification from the spectrograph slit to the detector pixel size, as well as the total length of slit determine the spectrograph parallel beam size and thus the overall size of the optical system.

For a large number of spectra, a wide-field optical system is typically required. Such optical systems are challenging in terms of technical feasibility (controlling optical aberrations), and cost. As an example, Figure 1.9 shows the layout of the PMAS (Potsdam Multiaperture Spectrophotometer) spectrograph optics, which is optimized to cover the wavelength range 350–900 nm (Roth *et al.*, 2005). It is worthwhile noting that the lens sizes are 200 mm in diameter. While this size represents the state-of-the-art for modern

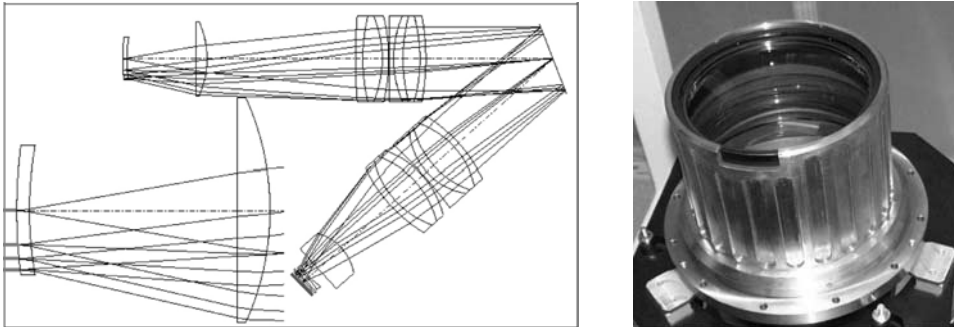


FIGURE 1.9. PMAS fiber spectrograph as an example for an IFS optical system. Left: a cross section, showing the layout of collimator, grating and camera. The parallel beam measures 150 mm in diameter. The magnified detail to the lower left illustrates the fiber interface. Right: photograph of the camera, which has a total mass of 60 kg.

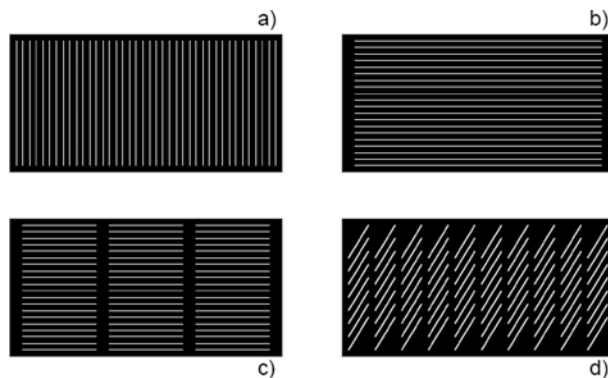


FIGURE 1.10. Different ways of allocating spectra on a detector: a) maximizing number of spaxels with full wavelength coverage, b) maximizing number of spectral pixels, c) maximizing number of spaxels with several banks of spectra, d) diagonal, maximizing number of spaxels at expense of wavelength coverage.

refractive optical systems for spectroscopy, the apochromatic correction from the ultra-violet (UV) to the NIR is unusual and quite demanding. The cost of such a system is high, mainly because of the use of expensive materials, e.g. CaF_2 , which are required for high throughput and the large wavelength coverage. Instruments that are not designed for general-purpose operation but rather for a specific science case can often be built simpler and with less effort.

Given the total number of spaxels of the IFU, the critical question of how to allocate the corresponding spectra on the detector arises. Obviously, the total number of detector pixels is related to the number of spatial and spectral resolution elements like:

$$\Sigma_{\text{Pixels}} \geq N_{\text{Spaxels}} \times N_{\text{Spectra}} \quad (1.1)$$

In most conventional 3D spectrograph designs the detector space is not contiguously filled with spectra, basically in order to avoid cross-talk between adjacent spectra and to facilitate data reduction. Novel slicer designs like, for example, SINFONI (Eisenhauer *et al.*, 2003) or the OSIRIS lens array IFU (Larkin *et al.*, 2006) have, however, demonstrated that this is not a necessary condition. Figure 1.10 shows several basic ways of arranging the spectra. Generally, a trade-off needs to be made between maximizing the number of spaxels, or the number of spectral pixels.

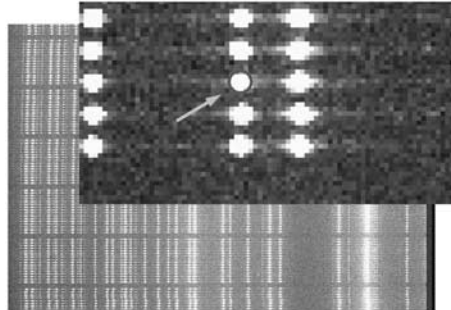


FIGURE 1.11. Typical CCD frame of an arc lamp exposure from a fiber bundle IFU. The direction of dispersion is horizontal. The magnified insert demonstrates how the instrumental profile is given by the FWHM (full-width-at-half-maximum) of the projected fiber size on the detector (≈ 4 pixels).

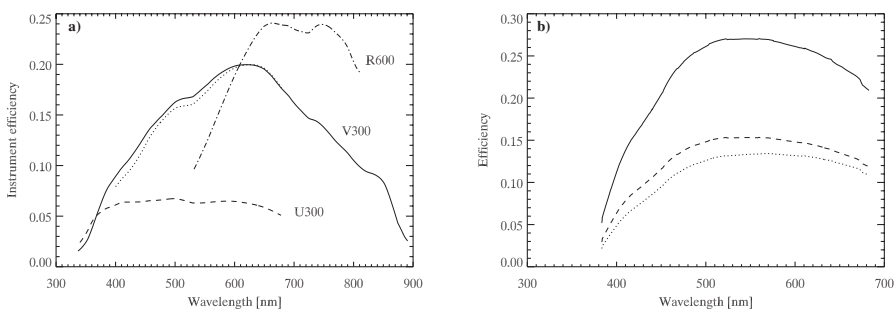


FIGURE 1.12. Examples for instrumental efficiency as a function of wavelength for different gratings. a) PMAS with lens array IFU, b) PMAS with PPAk IFU.

Spectral resolution and wavelength coverage

The spectral resolution in most 3D instruments does not reach the diffraction limit. It is rather determined by the projected (pseudo-)slit width on the detector. Figure 1.11 illustrates this situation with an example dataset, which was obtained with a fiber-based 3D spectrograph.

As mentioned before, the wavelength coverage is normally tuned to the application and scientific scope of an instrument. Two extreme examples on 4 m class telescopes would be:

- SAURON (WHT) [Spectrographic Areal Unit for Research on Optical Nebulae (William Herschel Telescope)], which has a wavelength coverage of 54 nm in the operational wavelength interval of 450–1100 nm; and
- PMAS (CAHA 3.5 m) [Potsdam Multiaperture Spectrophotometer], with a wavelength coverage of up to 680 nm in the interval of 350–900 nm. Instrumental efficiency curves for the latter instrument are given in Figure 1.12.

Coupling the IFU to the spectrograph

Although this is a somewhat technical detail, it is worth pointing out the fundamental difference between two different methods of coupling the IFU to the spectrograph optical system. One method is the one that has conventionally been used for normal slit-based spectrographs, namely to image the (dispersed) telescope focal plane (= slit) onto the detector. This technique is normally used for the ‘image slicer’ type of 3D spectrograph.

TABLE 1.2. Examples for 3 types of 3D spectrographs

	N_{spectra}	FoV ["]	scale ["]	R	λ range/ $\Delta\lambda$ [nm]
SAURON LR	1577	41×33	0.94	1200	450–700/54
SAURON HR	1577	11×9	0.27	1400	450–700/54
VIMOS LR	6400	54×54	0.67	220	370–1000/400
VIMOS HR	1600	13×13	0.33	2700	420–870/240
		8×8	0.25		
SINFONI	2048	3×3	0.10	1500–4000	1050–2450
		0.8×0.8	0.025		

Another method has emerged with the introduction of optical fibers in that the image information at the telescope focal plane is scrambled, and thus the one-to-one correspondence between points on the image plane and on the detector plane is lost. This principle is employed in an even more rigorous way in 3D spectrographs of the TIGER-type (TIGER = Traitement Intégral des Galaxies par l'Etude de leurs Raies; named after the prototype; Bacon *et al.*, 1995), where a simple fore-optics system followed by a lens array creates a tiny image of the entrance pupil (telescope aperture) for each lens. These so-called micropupils are designed to typically measure a few tens of micrometers in diameter. When fed to the collimator input plane of an imaging spectrograph, the family of micropupils practically operates like the apertures of a conventional multi-object spectrograph (e.g. the EFOSC-type), with the one significant distinction, namely that it is the telescope pupil rather than the telescope image that forms the multi-slit configuration. The important consequence is that the light distribution of the slit illumination no longer matters in terms of wavelength definition, which is an important argument for precision spectroscopy. The principle is not entirely new, but was first employed using a 'Fabry lens' for photoelectric photometers in order to eliminate the photometric noise introduced by seeing (Michlovic, 1972). Another variant of the TIGER micropupil technique is employed in fiber-optical 3D spectrographs, where the fiber bundle is connected to a lens array.

Examples of real IFUs

For the purpose of making the techniques introduced in the preceding sections more imaginable, three instruments are presented, which are meant to be representative for the (1) fiber-optical, (2) micropupil lens array (TIGER), and (3) slicer types of 3D spectrographs, namely the VIMOS (Visible Imaging Multi-Object Spectrograph; Le Fevre *et al.*, 2003), SAURON (Bacon *et al.*, 2001), and SINFONI instruments (Spectrograph for Integral Field Observations in the Near Infrared; Eisenhauer *et al.*, 2005). Some important parameters (number of spectra, FoV, spaxel size, spectral resolving power, wavelength coverage) are listed in Table 1.2 (LR/HR stand for low resolution and high resolution modes, respectively). Figure 1.13 shows examples of what the spectra look like on raw CCD frames for these three instruments. The VIMOS frame shows a science exposure from a stellar field, so some spectra are illuminated well, while most others contain only sky. Note that the direction of dispersion is oriented horizontally, and that the frame contains 4 banks of spectra that are placed as columns next to each other, with a gap between bank numbers 1 and 2. Note also that there are several artifacts as a result from zero and higher order contamination. The SAURON example shows a continuum flat-field exposure, which exhibits the characteristic pattern of the diagonal arrangement of the total 1577 spectra, whose density is so high that individual spectra are difficult to